AVERAGE GENUS OF ORIENTED RATIONAL LINKS

by

Dawn Ray

A dissertation submitted to the faculty of
The University of North Carolina at Charlotte
in partial fulfillment of the requirements
for the degree of Doctor of Philosophy in
Applied Mathematics

Charlotte

2022

Approved by:

_____
Dr. Yuanan Diao

_____
Dr. Gabor Hetyei

_____
Dr. William Brian

_____
Dr. Anthony Brizendine

ABSTRACT

DAWN RAY. Average Genus of Oriented Rational Links. (Under the direction of DR. YUANAN DIAO)

The goal of this dissertation is to develop the formulation of the average genus of all reduced alternating rational links and knots with a given crossing number. In 2014, Nathan Dunfield presented a preliminary report wherein he approximated the growth of the genus of knots with respect to the crossing number. His findings led him to hypothesize that this growth is linear [1]. Moshe Cohen recently submitted a paper providing a lower bound estimate of the average genus of knots with a given crossing number [2]. However, the actual average for knots and links has yet to be determined. Using the counting methods in a paper produced by Y. Diao, M. Finney, and D. Ray [3], we are able to derive a precise average for the genus of links and knots with crossing number given and estimate a weighted average of the genus for all rational links.

This dissertation consists of six chapters. Our most significant contribution and calculations are presented in chapters four and five after we familiarize the reader on the essentials of knot theory and its invariants and provide an overview of the results from our paper on enumerating rational links. The structure of the dissertation is organized as follows: in the first chapter, we provide a background of the field of knot theory as it relates to our results. The second chapter will familiarize the reader with definitions in knot theory as it pertains to our research. The next chapter will present the results from our enumeration paper including examples on how we addressed over counting and a walk-through of the construction of our computations. The fourth chapter will give specifics on how we were able to count the number of rational links with given crossing number based on the number of Seifert circles in the Seifert circle decomposition. In the fifth chapter we will discuss the theorems that will lay the final

foundational piece needed to determine the average genus and then discuss the final results. Lastly, the sixth chapter will discuss another type of link, the Montesinos link, and details how the results of our paper can be extended to future work in enumerating this special class of links.

ACKNOWLEDGEMENTS

Thank you to all those who made my dissertation possible. First and foremost, I would like to express my deepest gratitude to my advisor, Dr. Yuanan Diao for his patience and guidance through the research process. From the moment he agreed to be my advisor, he has been encouraging and selfless with his time and ideas. Without his guidance and help from the initial idea to the final proposal this dissertation would not have been possible. He has made himself available to me throughout these four years, which has helped me to develop an understanding and a deep appreciation of the subject.

I would like to thank my committee members, Dr. Gabor Hetyei for sharing all of his insights in our Knot Theory seminars, Dr. William Brian for his encouraging words and thoughtful questions, and Dr. Anthony Brizendine for agreeing to be on my committee and taking the time to learn about this fascinating field of study. I am truly fortunate that in the midst of all of the recent events and their activities they have accepted to be members of my dissertation committee.

Finally, I would like to thank my husband and children. They were always supportive, understanding, and patient with me through the duration of my studies here at the University of North Carolina at Charlotte. Most of all I want to thank my husband, I could not have done this without him.

TABLE OF CONTENTS

LIST OF TABLES

LIST OF FIGURES

CHAPTER 1: INTRODUCTION

The genus invariant is a geometric invariant of knots and links. In 1934 Herbert Seifert introduced an algorithm to create a connected orientable surface, known as a Seifert surface, from any given knot diagram. The genus of a link L is the *minimum* genus of any Seifert surface that spans L. In 1958 Richard Crowell and Kunio Murasugi both independently showed that by applying Seifert's algorithm to a reduced alternating diagram of an oriented alternating link one obtains a surface with minimal genus of that link [6], [7]. Formulations of the genus of 2-bridge, or rational, knots and links have been published but only in relation to polynomial invariants ([6], [7], [8], [9]). Recently Moshe Cohen used billiard table diagrams to determine a lower bound on the average genus of 2-bridge knots (a surface with only one component) with crossing number $c(D)$ [2]. In 2014 Nathan Dunfield used rejection sampling to compute upper and lower bounds on the average genus of rational knots when compared to the crossing number. His preliminary data indicated a linear relationship between the crossing number and the average genus [1]. In 2022 Cohen produced results that the average genus of a knot asymptotically approaches $c(D)/4 + 1/12$ [10].

We are particularly interested in determining the precise average genus for alternating rational knots and links with minimal diagram D and crossing number $c(D)$. It is known that we can use the formula $2g(L) = c(D) - s(D) - \mu(D) + 2$ to determine the genus of an alternating link diagram, where $s(D)$ is the number of Seifert circles and $\mu(D)$ is the number of components in D. In order to utilize this formula, there are two values we need to calculate to ascertain the average genus for rational links and knots with crossing number $c(D)$. First, in Chapter 4 we calculate the exact average

number of Seifert circles, $s(D)$, for all of the knots and links with crossing number $c(D)$. Second, we present theorems that allow for the differentiation between rational links ($\mu(D) = 2$) and rational knots ($\mu(D) = 1$). Our main result in Chapter 5 proves that this distinction is possible if we know $c(D)$ and $s(D)$. Using these two results, we are able to determine the average genus of links (knots) with given crossing number, $g^l_{c(D)}(D)$ ($g^k_{c(D)}(D)$). Further, we can estimate a general weighted average, $g_{c(D)}(D)$. Results from our data show a strong linear relationship between the average genus and the crossing number as $c(D) \to \infty$, a conjecture consistent with the results from Cohen [10].

Rational links are the closure of rational tangles. It is hypothesized that rational tangles play an important role in molecular biology in relation to the topology of DNA molecules. Enzymes that act on DNA during replication and recombination modify the structure of the helices to relieve super-coiling. During this process a substrate binds to the enzyme and the enzyme then performs an assigned action and releases a product. Observations of this process under electron micrography have produced pictures of DNA tangles that are converted into mathematical models of rational tangles. The role that the topology of these rational tangles play in DNA replication is not completely understood, but it is believed that particular configurations might serve a function.

An example from one particular experiment using the enzyme T_n3 resolvase shows several different links appearing throughout each step of the process of recombination. In this experiment the initial enzyme complex is an un-knotted DNA strand t_A, or the trivial knot. The substrate $N(t_s \bigoplus t_a)$ acts on t_A within the enzyme. During the first iteration in this process, the enzyme releases its product resulting in the Hopf link. The second iteration produces a figure-8 knot. After two subsequent products researchers were able to detect the 6_2 knot, as illustrated in Figure 1.1 [11].

Knot theory is a broad and deep subject with many classical problems and con-

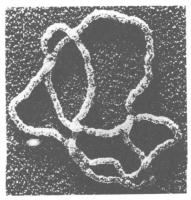

Figure 1.1: The DNA Knot 6_2 as a result of four rounds of recombination [4].

jectures. Enumerating links was one of the first challenges faced by knot theorists in its infancy. Peter Tait printed the first catalogue of knots in 1876 and in 1987 Claus Ernst and DeWitt Sumners obtained a precise formula for the number of un-oriented rational links. Readers interested in the history of enumeration can refer to [12], [13], [14], and [15]. Our paper [3], the results of which are summarized in Chapter 3, completely enumerates the oriented rational links with crossing number $c(D)$ using an invariant called the deficiency number. To do this we define a particular representation of the Seifert circle diagram, called a R-template. We use this template as a foundation for our results in Chapters 4 and 5, and as a result we are able to determine the average genus of all rational knots and links.

Our future work will consist of applying our enumeration techniques to a larger class of links called the Montesinos links.

CHAPTER 2: DEFINITIONS

In this chapter, we will discuss background information needed to understand the subsequent chapters. We begin with definitions in topology as it relates to surfaces and genus, we will then describe key concepts within knot theory and introduce the rational tangle and detail the importance of this tangle as it relates to our research. Finally, we will define and discuss specific invariants used in our research.

2.1 Seifert Surfaces and Genus

A *n-manifold* is a topological space X in which each point $x \in X$ has a neighborhood U that contains x and is homeomorphic (or topologically equivalent) to $\mathbb{R}^n$. If X has a boundary, and $x \in U$ maps to a point on the boundary, then x is a boundary point. The set of all boundary points in X is called the boundary of X. X is *compact* when any covering of X by open sets has a finite subcover [16]. A closed, compact manifold is a manifold with no boundary. Our main interest lies in compact manifolds of dimensions 1 and 2. A *surface* is a compact 2-manifold.

A surface F is *orientable* if every point in F can be consistently associated with a clockwise or counter-clockwise direction. Surfaces that are not orientable are referred to as *unorientable*. One of the most-well known unorientable surfaces is the Möbius band, illustrated in Figure 2.1 below. For our purposes we will only be interested in orientable surfaces. The Classification Theorem for Compact Surfaces states that every oriented compact surface is homeomorphic to a sphere or a connected sum of tori [17], thus we are able to classify any orientable surface.

A function f mapping topological spaces $f : X \to f(X) \subset Y$ is a *homeomorphism* if f and f^{-1} are continuous and f is a bijection. Further, we say f is an *embedding*

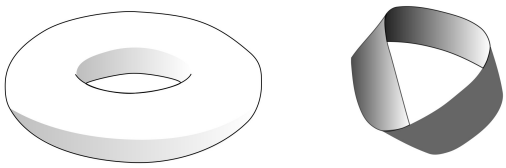

Figure 2.1: Left: A surface with orientation (torus), Right: An unorientable surface (Möbius band)

and X is embedded in Y.

A *homotopy* of a topological space $X \subset \mathbb{R}^3$ is a continuous map $f : X \times [0,1] \to \mathbb{R}^3$. Let $t \in [0,1]$ with $f_t(X)$ representing the evolution of X at any given time, t, and f_0 be the identity map. We define the mapping as an *isotopy* if f_t is injective for all $t \in [0,1]$ [16]. A *genus* is the number of holes or handles that a surface has. A torus is a surface of genus 1. Figure 2.2 is an example of a surface with genus 2.

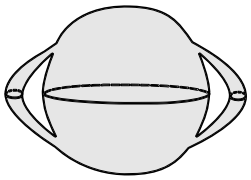

Figure 2.2: A surface with genus 2

2.2 Knots and Links

A *knot* $K \subset \mathbb{R}^3$ is the embedding of a unit circle S^1 into Euclidean 3-space, $\mathbb{R}^3$. A *link* is a finite disjoint union of knots: $L = K_1 \cup K_2 \cup .... \cup K_n$, where each K_i is called a *component* of the link. Two knots are identified as *equivalent* when carrying out certain moves in 3-space doesn't damage or change the essential topological properties of the knots. Two knots K_1 and K_2 are *ambient isotopic* if there is an isotopy $h : \mathbb{R}^3 \times [0,1] \to \mathbb{R}^3$ such that h_0 is the identity map, and each h_t is a homeomorphism for $t \in [0,1]$. Thus two knots are equivalent if they are ambient isotopic.

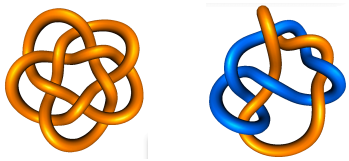

Figure 2.3: Presentations of a knot (left) and a link (right) in $\mathbb{R}^3$.

The projection of a knot onto a two-dimensional plane gives a planar representation of the knot called a *knot projection* or a knot diagram. Let $\pi : \mathbb{R}^3 \to \mathbb{R}^2$ be the mapping of the projection of a knot $K \subset \mathbb{R}^3$. We say a point $x_1 \in \pi(K))$ is a *multiple point* if a neighborhood U around $\pi^{-1}(x_1)$ contains more than one element. The projection of a knot is called *regular* if there are a finite number of multiple points and all such points are double points, known as *crossings*. In other words, $|\pi^{-1}(x)| \leq 2$ for all $x \in \pi(K)$ and $|\pi^{-1}(x)| = 2$ for a finite subset of $x \in \pi(K)$. Projections of almost all knots and links, with the exception of the *wild* knots, have a regular projection.

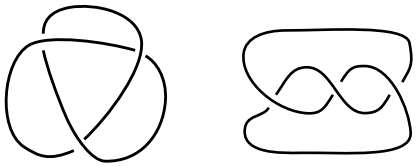

Figure 2.4: Two presentations of the knot projection of the trefoil knot.

Let D be the regular planar diagram of a link L. As shown in Figure 2.4, this diagram D has breaks at each crossing to indicate an over and under strand. We can give the link L orientation by choosing a direction to traverse the link. If the link L is oriented, then D will inherit this orientation. Each crossing is given a sign based on the direction of the over strand. A crossing is defined as *positive* if it is presented as the left crossing in Figure 2.5 and negative otherwise.

Equivalent planar diagrams have many different presentations. For example, Figure

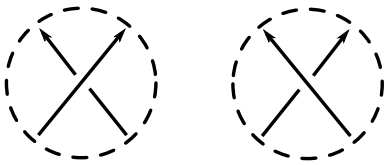

Figure 2.5: Example of a positive and negative crossing in D

2.4 shows two equivalent presentations of the trefoil knot. Let D_1 and D_2 be regular projections representing a link L. Then there exists a finite sequence of moves, called *Reidermeister moves* that will take D_1 to D_2. Performing these moves on a link diagram allows for manipulation of a projection while preserving the link type. There are three types of Reidermeister moves as illustrated in Figure 2.6. Type 1 (R_1) adds or removes a curl, type 2 passes one string over another, and type 3 pushes one strand past a crossing involving two strands. Reidermeister proved that these three moves in conjunction with a planar isotopy are all that is required to transform D_1 to D_2 [18]. Since each of these operations can be realized via an ambient isotopy to the link, equivalent diagrams define equivalent links [19].

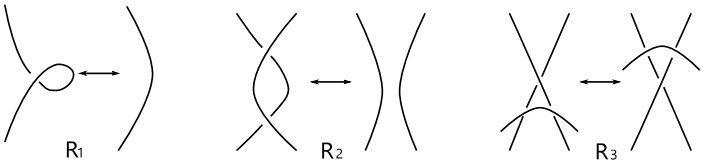

Figure 2.6: Reidermeister moves

A projection is *alternating* when traversing the knot results in each over crossing subsequently followed by an under crossing and vice versa. Most links are non-alternating, however alternating links are a very important class of links with several nice properties. Crossings that can be removed by a simple twist are called *nugatory*, see Figure 2.7. A diagram with no nugatory crossings is called a *reduced* diagram.

Let D now be a reduced, alternating projection of a link L. By choosing an

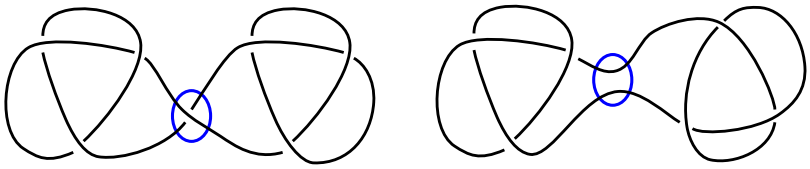

Figure 2.7: Removing a nugatory crossing.

orientation for each component, at each crossing we will create a small neighborhood and make a local change as shown in Figure 2.8: first delete the crossing and then connect the two compatible ends based on their orientation. We continue to do this at each crossing, resulting in a series of disjointed loops in $\mathbb{R}^2$ with no crossings. These loops are called *Seifert circles*. The collection of all Seifert circles in D is called the *Seifert circle decomposition* of D. Note that some Seifert circles may be nested. Let $s(D)$ be number of Seifert circles in D.

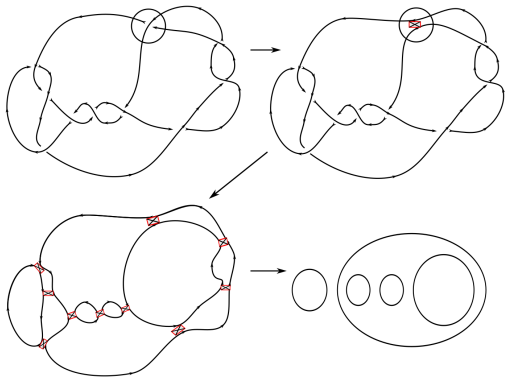

Figure 2.8: A neighborhood of a crossing (top left) shown with the crossing smoothed based on their orientation (top right). Smoothing all crossings (bottom left) results in the Seifert circle decomposition (bottom right)

A *Seifert graph* G is constructed by associating each Seifert circle with a vertex and each edge with their shared crossing(s). Each edge can be labelled with a $+$ or $-$ to indicate the sign of the associated crossing in D. A single edge between two circles indicates a *single* or *lone* crossing. Two vertices that share more than one edge

represent two Seifert circles that share *multiple* crossings. A *cycle* is a circuit with $2n$ vertices. In Figure 2.9, the Seifert graph of the 10_{12} knot shows the Seifert circle decomposition has five Seifert circles including a 4-cycle with three lone crossings and one multiple crossing.

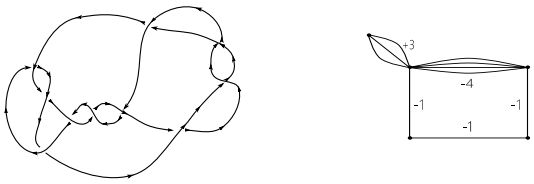

Figure 2.9: A planar representation of the 10_{12} knot with orientation and its associated Seifert graph.

A *Seifert surface* of a link L is an orientable surface S embedded in $\mathbb{R}^3$ with L as its boundary. Given a projection of a link, we can create a Seifert surface as follows: placing the projection on the xy-plane, we will perform the operations to create a Seifert circle decomposition. Each circle in the decomposition will then be made to bound a disc in the plane. We will place the circles at different heights in the z-plane so that no circle will lie on the same horizontal plane. Each crossing will be presented as twisted bands that will connect the discs to one another. The resulting surface will have one boundary component so that the boundary component is the link [20].

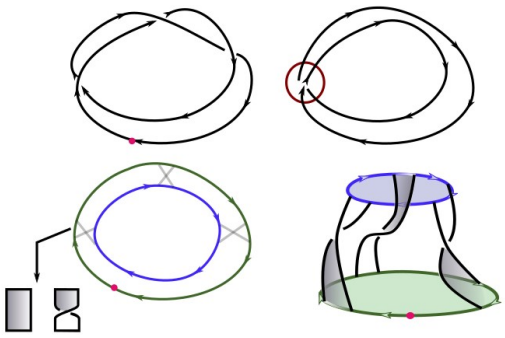

Figure 2.10: Creation of a Seifert surface from a projection of the trefoil knot.

The *genus* of a link L is the minimal genus among all Seifert surfaces of L [19]. We will denote $g(L)$ as the genus of L. The genus of L is an *invariant*. Invariants are constants or polynomials that are intrinsically associated with a link. If two links are equivalent, then their invariants will be equal. However equality of invariants does not guarantee link equivalence.

The genus of a projection surface of L constructed from D satisfies the equation $2g(L) = c(D) - s(D) - \mu(D) + 2$ where $\mu(D)$ is the number of components in D. However, a minimal crossing diagram does not guarantee the construction of a minimal genus surface. There are some knots where it is impossible to construct a minimal genus spanning surface on any diagram.

2.3 Rational Tangles

A *tangle*, T is a region in the projection plane surrounded by a circle. Four strings protrude from T in the four intermediate directions. A *rational tangle* or a 2-tangle, lies within the circle and is constructed by alternatively twisting the ends in a series of vertical/horizontal twists. The tangle is referred to as $(a_1, a_2, ..., a_n)$ where each a_i, $1 \leq i \leq n$ represents the number of twists. For example in Figure 2.11, we have a rational tangle presented as $(3, 2, 2)$. Rational tangles are classified by relating them to loops on a torus and in so doing we can associate them with a pair of coprime integers (p, q) [16]. The rational tangle is thus referred to as the p/q-tangle.

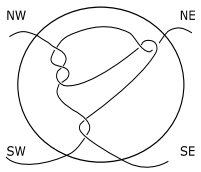

Figure 2.11: An example of a p/q tangle on the projection plane.

A *rational link* can be formed by connecting the loose ends of the tangle. There are several ways to represent a planar diagram of a rational link. We can perform a

numerator or denominator closure on the tangle, in which neighboring loose ends are joined together, an example of which is shown on the left in Figure 2.12. They can also be presented as a braid or plat closure (Figure 2.12 (right)) with four strings. This presentation is also known as a 4-plat, or a 2-bridge, link [21]. These representations are equivalent, as can easily be seen between the rational link and 4-plat in Figure 2.12, by performing a planar isotopy.

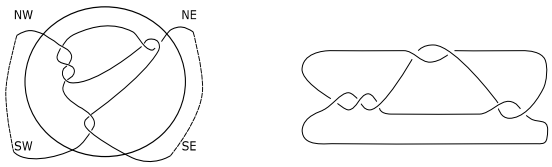

Figure 2.12: Left: Denominator closure of the $(3, 2, 2)$ rational tangle results in a link. Right: equivalent representation of the $(3, 2, 2)$ link as a braid.

Let $L = d(p, q)$ be the denominator closure of a rational link, where p and q are co-prime integers and $0 < p < q$. Let the components of the odd-lengthed vector $(a_1, a_2, ..., a_{2n+1})$ represent the twists in the rational tangle. We can represent the vector as a continued fraction decomposition with each $a_1 > 0$ and

$$\frac{p}{q} = \frac{1}{a_1 + \frac{1}{a_2 + \frac{1}{....+a_{2n}+\frac{1}{a_{2n+1}}}}}.$$

Under these given conditions the continued fraction decomposition is unique [22].

In 1956 Shubert presented two very important results proving the equivalence between rational links [23]. The first is that two unoriented links $d(p, q)$ and $d(p', q')$ are topologically equivalent if and only if i) $q = q'$ and ii) either $p = p'(\text{mod}q)$ or $p \cdot p' = 1(\text{mod}q)$ [23]. The second states that two oriented links are topologically equivalent if and only if i) $q = q'$ and ii) either $p = p'(\text{mod}2q)$ or $p \cdot p' = 1(\text{mod}2q)$ [23].

2.4 Braids and Additional Invariants

A cylindrical n-tangle is a ball $D^2 \times [0,1]$ with a series of n-inputs descending from the top ($D^2 \times 1$) and a line of n-outputs in the bottom directly below [16]. A cylindrical n-tangle is called a *n-string braid* if it has no extra loops, and each string does not intersect others and descends monotonically, that is, without reversing direction.

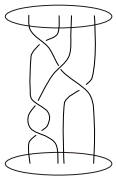

Figure 2.13: A 4-string braid

A closed braid is formed when the two discs are glued together. It is known that every oriented link can be presented as the closure of a braid [24]. The *braid index* $b(L)$ of a link L, is another knot invariant. It is the minimum number of strings needed to present a link as a closed braid from all possible projections of L. Similar to the genus, the braid index requires the minimization of a geometric property, so it can be very difficult to calculate. Let $\tilde{s}(L)$ represent the minimal number of Seifert circles for all possible Seifert circle diagrams of L. In 1987, Yamada proved that for any oriented link, $\tilde{s}(L) = b(L)$ [25]. In 1993, Murasagi and Przytycki proved there was a systematic way to reduce the number of Seifert circles to their minimal value using a link preserving operation (M-P operation). The foundation of this operation reroutes lone crossings in a cycle of Seifert circles. Note that lone crossings can only occur in cycles, otherwise they would be nugatory. By systematically rerouting any existing single, non-nugatory crossings, cycles are reduced and eventually collapse into a Seifert graph with no cycles. Once all the cycles have been removed, the minimal diagram has been obtained. The authors conjectured (M-P conjecture) that the braid index may be equal to the number of Seifert circles in D minus the maximal number

of M-P operations.

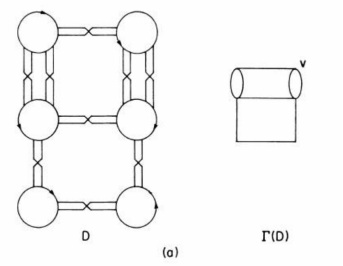

Figure 2.14: A Seifert decomposition with six Seifert circles, two 4-cycles and corresponding Seifert graph [5]

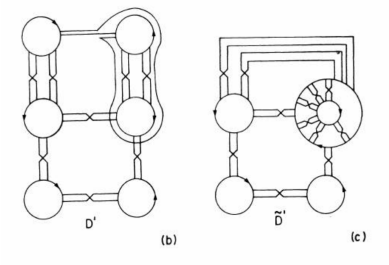

Figure 2.15: A single crossing in the top 4-cycle is rerouted and reduces the number of Seifert circles to four. [5]

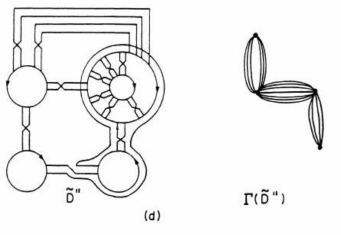

Figure 2.16: Another lone crossing is rerouted reducing the second cycle resulting in a reduced diagram with no lone crossings and its associated reduced Seifert graph [5]

Using the M-P operation, Diao, Hetyei and Liu proved that, for a reduced alternating diagram D of an alternating link L, $b(L)$ equals the number of Seifert circles $s(D)$ if and only if the Seifert graph has no edges of weight one (no lone crossings)

[26]. They further proved that the M-P conjecture was in fact true for many reduced alternating diagrams including all rational links and alternating Montesinos links. The *reduction* number $r(D)$ is defined as the maximum number of Seifert circles that can be reduced by rerouting lone crossings in D. In [27] Diao, Ernst, Hetyei, and Liu proved for several classes of links that $b(D) = s(D) - r(D)$.

Consider two links L_1 and L_2 and their projections D_1 and D_2, these two links can be summed by cutting into each link and reconnecting the ends, as illustrated in Figure 2.17. This construction is called the *connected sum* operation and is denoted $L_1 \# L_2$. A long conjectured question in knot theory is whether the crossing number of a link is additive under the connected sum operation, in other words is it true that $c(L_1) + c(L_2) = c(L_1 \# L_2)$. The answer is known for several classes of links, but not for all. To prove this conjecture is true for the torus knots, Diao defined an invariant called the deficiency number $d(L)$ of a link L as $d(L) = c(L) - 2g(L) - b(L) - \mu(L) + 2$ [28]. Furthermore, he proved that for links with deficiency zero ($d(L) = 0$) the connected sum equality holds. Using the results from [27] and the definition of genus, $2g(L) = c(D) - s(D) - \mu(D) + 2$ we can now redefine the deficiency number. For a reduced alternating link L and its associated planar diagram D, it is known that $g(D) = g(L)$, $c(D) = c(L)$, and $\mu(D) = \mu(L)$. Thus a simple substitution results in $d(L) = (2g(L) + s(D) + \mu(D) - 2) - 2g(L) - b(L) - \mu(L) + 2 = s(D) - b(L)$. Since $b(L) = s(D) - d(L)$, a link is of deficiency zero only if $b(L) = s(D)$. Finally we can see from our definition of the reduction number that $d(L) = r(D)$.

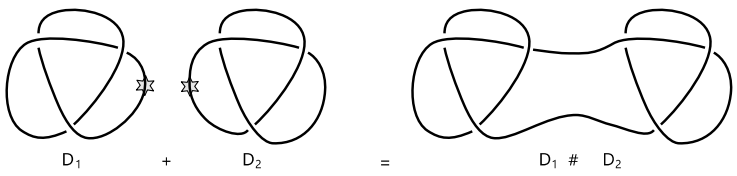

Figure 2.17: Projections of the connected sum of two trefoil knots L_1 and L_2

Using the reduction (deficiency) number and the results summarized in this section,

we will next present how we were able to enumerate the set of oriented rational links with a given deficiency number.

CHAPTER 3: ENUMERATION OF RATIONAL LINKS

In this chapter, we will discuss the results from our paper [3] which details how to enumerate the oriented rational links, for a more detailed reading, we refer the reader to Diao, Finney, and Ray [3]. Note that in the following discussion that the usage of the word knot specifically indicates a link with only one component while a link can have one or more components.

The challenge of enumerating links and knots is a classic problem in knot theory. Peter Tait was the first mathematician to print a catalog of knots in 1876. It contained the diagrams of 15 knots with up to 7 crossings. In 1885, Charles Little created a more extensive catalog of alternating links up to order (crossing number) 10 and then took an additional six years to create a catalog of non-alternating diagrams with up to 10 crossings. This list, done all by hand, had no omissions and only one duplication (left undiscovered until 1974) [14]. In the 1960's John Conway introduced the concept of the tangle. Using this powerful notation, he was able to enumerate knots up to order 11 and links up to order 10 with only 4 omissions. This ended the era of hand calculation. In the 1980's Dowker and Thistlethwaite used computers to extend the catalog to 13 crossings. And in the 1990's Thistlethwaite extended the list to order 16, a catalog of over 1.7 million knots. [16]

The discovery of invariants has been an invaluable tool in the advancement of solving the enumeration problem for links with n crossings. In 1987, Ernst and Sumners were able to define a precise formula for the set of un-oriented rational links $|\mathcal{U}_n|$ with crossing number n [15].

$$|\mathcal{U}_n| = 2^{n-3} + 2^{\lfloor \frac{n-3}{2} \rfloor}$$

Using their calculation of un-oriented rational links, in our paper Diao formulated the count of the oriented rational links, Λ_n as [3]

$$|\Lambda_n| = \frac{1}{3}\left(2^{n-1} + \frac{5+(-1)^n}{2}2^{\lfloor\frac{n}{2}\rfloor-1} + \frac{-1+(-1)^n+2(-1)^{\lfloor\frac{n+1}{2}\rfloor n}}{2}\right)$$

Using the Seifert circle decomposition of a rational link and the reduction number invariant, the purpose of this chapter is to show how to get a precise count of the number of oriented rational links.

3.1 Preferred Standard form and R-Decompositions

Let $p, q \in \mathbb{N}$ with $0 < p < q$ and $\gcd(p, q) = 1$. Let $a_1, a_2, ... \in \mathbb{Z}^+$ and $(a_1, a_2, ..., a_{2k+1})$ be the unique vector of odd length such that

$$\frac{p}{q} = \frac{1}{a_1 + \frac{1}{a_2 + \frac{1}{\cdots \frac{1}{a_{2k} + \frac{1}{a_{2k+1}}}}}}.$$

The above will be presented as $p/q = [a_1, a_2, ..., a_{2k+1}]$. The rational link corresponding to p/q will be presented as the 4-plat projection $\mathcal{L}$ where each a_j represents crossings in the 4-plat. Labelling the strings of the 4-plat I-IV from top to bottom as shown in 3.1, we will begin with a_1 representing leftmost crossings between strings II and III and shift up to strings I and II for crossings a_2, then down to strings II and III for a_3 and so on. This pattern will continue until we reach a_{2k+1}, the rightmost crossing, between strands II and III. We will refer to this projection as being in *preferred standard form* (or PS form) if the link is drawn so that the bottom string of the 4-plat is oriented from right to left and the first crossing on the left (a_1) is an under crossing with respect to the long strand (string IV) at the bottom.

Given a projection $\mathcal{L}$ in the PS form, we will define the *reversal* of the 4-plat to be the 180 degree rotation around a vertical axis and the changing of the orientation of the component(s). The reversal will result in a 4-plat $\mathcal{L}'$, see Figure 4.2. Rational

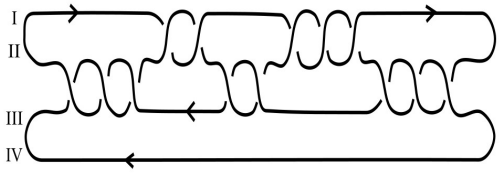

Figure 3.1: The rational link (56/191) presented in the PS form with strings labelled.

links where $\mathcal{L}$ and $\mathcal{L}'$ are indistinguishable are called *symmetric*. The reversal of a 4-plat is equivalent to the inverse of $\mathcal{L}$. Since rational links are invertible, we know that $\mathcal{L}'$ is equivalent to $\mathcal{L}$, thus $\mathcal{L} \sim \mathcal{L}'$.

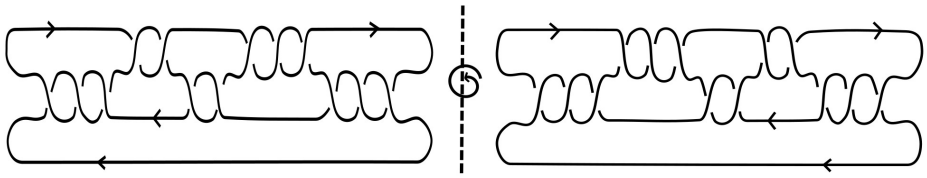

Figure 3.2: The rational link $\mathcal{L}$ and its reversal $\mathcal{L}'$

Using Shubert's results [23], we proved that every oriented rational link $\mathcal{L}$ can be presented as at most two 4-plats in the PS form [3]. In the case that the projection of $\mathcal{L}$ in the PS form can be represented by exactly two distinct projections, then these two rational links must be the reversals of each other.

A rational link can only have one or two components and $\mathcal{L}(p/q)$ will have two components if and only if q is even. If it has one component, then q is odd and the sign of the first crossing a_1 is determined by the designated orientation given by the definition of the PS form. If it has two components, the first crossing will be positive or negative based on the orientation of the second component, which will be determined by the orientation of the top strand.

The Seifert circle decomposition of an oriented rational link in PS form will be called an *R-decomposition*. Let the Seifert circle C created by the long arc on the bottom be called the *large Seifert circle*.

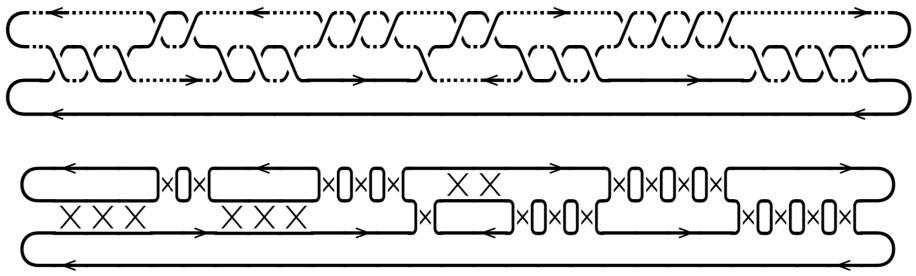

Figure 3.3: Top: The rational link $[3, 2, 3, 3, -1, -2, -3, 4, -4]$ with orientation; Bottom: the associated R-decomposition

Assigning orientation of the component(s) will result in a signed vector $[b_1, b_2, ..., b_{2m+1}]$ where each $b_i = \pm a_i$ corresponds to the sign of each a_i crossing. For example, Figure 3.4 shows $\mathcal{L}(5075/17426)$ with orientation resulting in the signed vector $[3, 2, 3, 3, -1, -2, -3, 4, -4]$. We can now group consecutive b_j's with the same signs together, which will result in a series of *blocks*, which we will denote as $B_1, B_2, ...$ One can see that positive crossings reside outside of C while negative crossings are inside C. This can be further clarified into the statement: positive blocks result in Seifert circles outside of C and negative blocks result in Seifert circles inside of C. In Figure 3.4, the R-decomposition shows blocks $B_1 = (3, 2, 3, 3)$, $B_2 = (-1, -2, -3)$, $B_3 = (4)$, and $B_4 = (-4)$

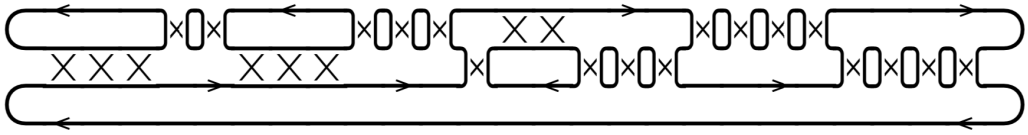

Figure 3.4: R-decomposition of $[3, 2, 3, 3, -1, -2, -3, 4, -4]$ with the shown orientation of $\mathcal{L}(5075/17426)$

3.2 Rational Links Types and Addressing Over Counting

Since $\mathcal{L} \sim \mathcal{L}'$ and each non-symmetrical link $\mathcal{L}$ and $\mathcal{L}'$ have distinct PS forms and thus distinct Seifert circle decompositions, we have to address the over-counting that will naturally occur when enumerating the oriented rational links. To do this, we will

break up the links into four possible vector block arrangements. We will refer to these as Types. We will define Type I rational links as links that have an even number of blocks where the first block is positive (and thus last block is negative). A Type II link will have an even number of blocks with a negative first block.

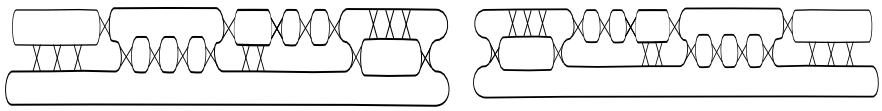

Figure 3.5: Top: Example of a Type I (left) R-decomposition and (right) a Type II

Conversely the Type III links will have an odd number of blocks, with a positive first block (and positive last block) and Type IV will also have an odd number of blocks, but with a negative first block.

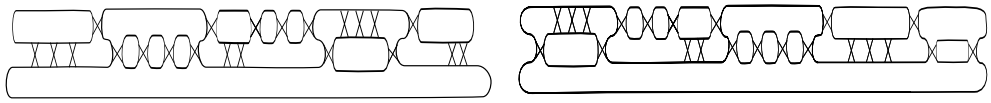

Figure 3.6: Top: Example of a Type III (right) rational link and (left) a Type IV

We use R_n^I, R_n^{II}, R_n^{III} and R_n^{IV} to denote the sets of rational links with R-decompositions of Type I, II, III, IV. Additionally, we will use RS_n^I, RS_n^{II}, RS_n^{III} and RS_n^{IV} to correspond to the subset of links that are symmetric with respect to the reversal operation.

The reversal of a Type I (Type II) results in a Type II (Type I) As can be seen by looking at the R-decomposition in Figure 3.5. Since there are an even number of blocks there are no Type I or II symmetrical links, thus $RS_n^I = RS_n^{II} = \emptyset$. The reversal of a Type I will always result in a Type II, and therefore there is a one-to-one correspondence between the Type I and Type II R-decompositions, or equivalently $|R_n^I| = |R_n^{II}|$.

The reversal of a Type III (Type IV) 4-plat remains a Type III (Type IV) 4-plat. This is also true of the Type III (IV) symmetric links. However, when we take the

mapping of a (symmetric) Type III 4-plat to its mirror image, there is a one to one correspondence between the (symmetric) Type III and (symmetric) Type IV 4-plats, thus $|R_n^{III}| = |R_n^{IV}|$ and $|RS_n^{III}| = |RS_n^{IV}|$

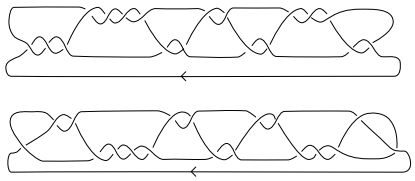

Figure 3.7: The rational link with signed vector $[3, 4, -2, -2, -2, 3, 2]$ (Top) is of Type III. (Bottom) The mirror image $[-1, -2, -4, 2, 2, 2, -3, -1, -1]$ (Bottom) is a Type IV.

Let Ω_n be the set of all R-decompositions with crossing n. Since $|R_n^I| = |R_n^{II}|$ and $|R_n^{III}| = |R_n^{IV}|$, then

$$|\Omega_n| = |R_n^I| + |R_n^{II}| + |R_n^{III}| + |R_n^{IV}| = 2|R_n^I| + 2|R_n^{III}|$$

and since $|RS_n^{III}| = |RS_n^{IV}|$, let Ω'_n be the set of all symmetric R-decompositions then

$$|\Omega'_n| = |RS_n^{III}| + |RS_n^{IV}| = 2|RS_n^{III}|$$

Let Λ_n be the set of all oriented rational links presented in PS form with crossing number n. Since each link and its reversal reside in the set $|\Omega_n|$ and $|\Omega'_n|$, then

$$|\Lambda_n| = \frac{|\Omega_n| + |\Omega'_n|}{2}$$

and therefore

$$|\Lambda_n| = |R_n^I| + |R_n^{III}| + |RS_n^{III}|.$$

3.3 Enumeration of Rational Links using the Reduction Number

We will now further define specific Seifert circles in the R-decomposition of $\mathcal{L}(p/q)$. We have already defined C as the large Seifert circle. A *medium* Seifert circle will be a Seifert circle that may share at least one crossing with C. A Seifert circle that cannot share any crossings with C will be referred to as a *small* Seifert circle. Thus, a small Seifert circle will share single crossings on both sides with medium Seifert circles, but will not share a crossing with C.

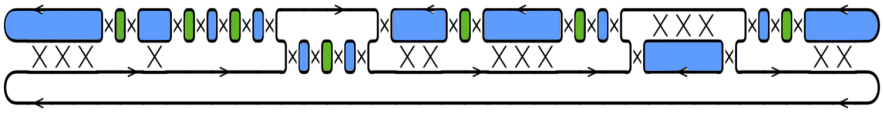

Figure 3.8: R-decomposition with Seifert circles identified. Medium Seifert circles appear in blue and small Seifert circles appear in green.

We define a *reduction operation* as the removal of a small Seifert circle and combining its two neighboring medium Seifert circles into a single medium Seifert circle, see Figure 3.9 (left). The *deficiency*, d, is defined as the total number of reduction operations one can perform on $\mathcal{L}$.

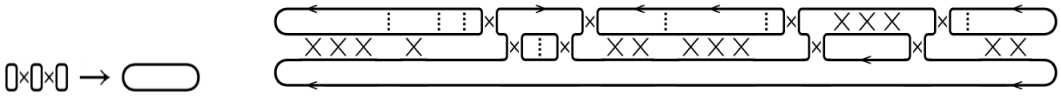

Figure 3.9: A reduction operation on a rational link in PS form combines three small Seifert circles into one medium and removes two crossings (left). (Right) The result of all reduction operations performed upon Figure 3.8. Dashed lines indicate where each reduction operations occurred.

The crossings deleted by the reduction operation will be referred to as *r-crossings*. Performing each reduction operation will reduce a small Seifert circle and consequently the number of r-crossings will decrease by two. Once all reduction operations are performed, the R-decomposition will be of deficiency zero and will consist of C

and medium Seifert circles see Figure 3.9 (right). The first and last crossing that each medium Seifert circle shares with the C will be called *essential crossings*. The crossings that are not essential will be called *free crossings*.

A *R-template* is a R-decomposition with zero deficiency and no free crossings. A R-decomposition with deficiency d and f free crossings can be reduced to a R-template by performing reduction operations and removing all the free crossings. Reversing this process, we can reconstruct a R-decomposition starting with its R-template. For example, we can construct the R-decomposition of the link in Figure 3.9 by using a R-template with five medium Seifert circles. Since $d = 7$, we will perform 7 insertions by inserting small Seifert circles and their associated r-crossings in the locations indicated by the dashed lines. We can then place the free crossings to complete the R-decomposition. R-templates that contain k medium Seifert circles will have $2k$ essential crossings. The deficiency d represents the insertion of a small Seifert circle, and each insertion results in the addition of two r-crossings. Thus a R-decomposition with k medium Seifert circles and deficiency d will have a total of $n = f + 2d + 2k$ crossings.

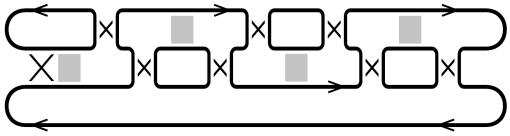

Figure 3.10: Example of an R-template with eight essential crossings and four medium Seifert circles.

We can now refer back to the signed vector notation in Section 3.1 and note that the number of blocks relates directly to k, the number of medium Seifert circles in a R-template. Thus we can say that a R-template of a Type I link will have $k = 2j$-medium Seifert circles ($j \geq 1$) and a Type III (symmetric) will have $k = (1 + 2j)$-medium Seifert circles.

3.4 Counting the R-decompositions by Type

By definition, since a Type I link has $k = 2j$ medium Seifert circles, then the number of free crossings will be $f = n - 2d - 2k = n - 2d - 4j$ (where $n \geq 4$). The grey boxes in Figure 3.10 represent spaces where the free crossings can be distributed, and there are $2j$ of these spaces. Thus there are $C(f + 2j - 1, 2j - 1)$ ways to distribute the free crossings. Once the free crossings have been placed, there are $f + 2j$ spots to insert small Seifert circles and there are $C(d + f + 2j - 1, f + 2j - 1)$ ways to perform the d insertions. From here it follows that [3]

$$|R_n^I(d)| = \sum_{j=1}^{\lfloor \frac{n-2d}{4} \rfloor} \binom{n - 2d - 2j - 1}{2j - 1} \binom{n - d - 2j - 1}{d}.$$

Using a similar argument for the Type III links, we have

$$|R_n^{III}(d)| = \sum_{j=0}^{\lfloor \frac{n-2d-2}{4} \rfloor} \binom{n - 2d - 2j - 2}{2j} \binom{n - d - 2j - 2}{d}.$$

The enumeration of the symmetric Type III rational links required us to address the nature of a symmetrical R-decomposition. In order to do this, we split the R-decomposition in half and discussed how we can distribute the free crossings and small Seifert circles on one side and the other half would have to fill in in a symmetrical manner. This resulted in four possible combinations of n and d. We encourage the reader to refer to our paper [3] for a detailed account, however these cases will be revisited in chapter 4, thus for the sake of brevity we will state only the resulting

formulation below.

$$
\begin{aligned}
& |RS_n^{III}(d)| \\
= & \begin{cases}
\sum_{j=0}^{\lfloor \frac{n-2d-2}{4} \rfloor} \binom{\frac{n}{2}-d-j-1}{j} \binom{\frac{n-d}{2}-j-1}{\frac{d}{2}}, & n \text{ even, } d \text{ even} \\
\sum_{j=0}^{\lfloor \frac{n-2d-2}{4} \rfloor} \binom{\frac{n}{2}-d-j-1}{j} \binom{\frac{n-d-1}{2}-j-1}{\frac{d-1}{2}}, & n \text{ even, } d \text{ odd} \\
\sum_{j=0}^{\lfloor \frac{n-2d-2}{4} \rfloor} \binom{\frac{n-1}{2}-d-j-1}{j} \binom{\frac{n-d-1}{2}-j-1}{\frac{d}{2}}, & n \text{ odd, } d \text{ even} \\
0, & n \text{ odd, } d \text{ odd}
\end{cases} \\
= & \frac{1+(-1)^{nd}}{2} \sum_{j=0}^{\lfloor \frac{n-2d-2}{4} \rfloor} \binom{\lfloor \frac{n}{2} \rfloor - d - j - 1}{j} \binom{\lfloor \frac{n-d}{2} \rfloor - j - 1}{\lfloor \frac{d}{2} \rfloor}.
\end{aligned}
$$

Table 4.2 contains the computational results of $|R_n^I(d)|$, $|R_n^{III}(d)|$, $|RS_n^{III}(d)|$ and $|\Lambda_n|$ for $2 \leq n \leq 13$.

Table 3.1: The three numbers in each (n, d) position are presented in the order $|R_n^I(d)|$, $|R_n^{III}(d)|$ and $|RS_n^{III}(d)|$.

n/d	0	1	2	3	4	5	$\lvert\Lambda_n\rvert$
2	0,1,1						2
3	0,1,1						2
4	1,1,1	0,1,1					5
5	2,1,1	0,2,0					6
6	3,2,2	2,3,1	0,1,1				15
7	4,4,2	6,4,0	0,3,1				24
8	6,7,3	12,8,2	3,6,2	0,1,1			51
9	10,11,3	20,18,0	12,10,2	0,4,0			90
10	17,17,5	34,37,3	30,21,5	4,10,2	0,1,1		187
11	28,27,5	62,68,0	60,51,5	20,20,0	0,5,1		352
12	45,44,8	116,119,5	115,118,10	60,45,5	5,15,3	0,1,1	715
13	72,72,8	212,208,0	228,246,10	140,116,0	30,35,3	0,6,0	1386

CHAPTER 4: ENUMERATION OF LINKS BASED ON SEIFERT CIRCLE AND CROSSING NUMBER

A Seifert surface for an oriented rational link (L) is an orientable surface whose oriented boundary is the link. The minimal genus of a Seifert surface of L is known as the *genus* and is denoted as $g(L)$. Let D be a reduced alternating link diagram of a link L. Let $s(D)$ be the number of Seifert circles in L and $g(D)$ be the genus of the Seifert surface constructed from the Seifert circle decomposition of D. It is known that $g(D) = g(L)$ and that Seifert's algorithm can be used to determine the minimal genus using the formula $2g(D) = c(D) - s(D) - \mu(D) + 2$, where $c(D)$ is the crossing number and $\mu(D)$ is the number of components in D. We are interested in finding the average genus of a reduced alternating rational link D for all rational knots and links with crossing number $c(D)$. In order to do this, we will need to first determine the average number of Seifert circles ($s(D)$) for each $c(D)$. This chapter discusses how we were able to determine that average.

4.1 Enumeration of the Type I links with Seifert circles s and crossing number $c(D)$

We will start by looking at the R-templates with an odd number of Seifert circles $s = 2j + 1$. Since there is always one large Seifert circle (C), this means we will have an even number ($2j$) of remaining (medium and small) Seifert circles.

Consider a R-template with no small Seifert circles. In Chapter 3 we defined the reduction operation as the removal of a small Seifert circle, we will now define an *insertion operation* as the addition of a small Seifert circle, see Figure 4.1. This operation will result in two medium Seifert circles with a small Seifert circle in between

them.

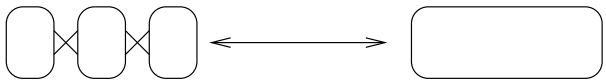

Figure 4.1: Insertion and reduction operations

Let $j = 1$. In this case, there is only one template option, since the insertion of a small Seifert circle into a medium Seifert circle would result in a total of 4 Seifert circles (C plus three other Seifert circles). Therefore the only possible R-template has two medium Seifert circles and one large Seifert circle C. We will call this a 3R-template as shown in Figure 4.2. Each medium Seifert circle will allow for the possibility of the insertion of free crossings and we define *insertion boxes* as the places where free crossings may be placed (shown as grey boxes in each R-template).

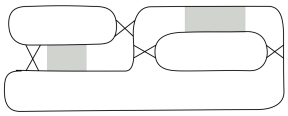

Figure 4.2: A 3R-Template shown with two insertion boxes

There will be $f = c(D) - 2(2j) = c(D) - 4$ free crossings and $b = 2j = 2$ insertion boxes to distribute the free crossings. This is the only configuration for a 3R-template. Let $\psi^I_{c(D)}(s)$ represent the total number of links of Type I with $c(D)$ crossings and s Seifert circles. We then have $\binom{b+f-1}{b-1=2+c(D)-4-12-1}$ possible ways to distribute free crossings, resulting in $\psi^I_{c(D)}(3) = c(D) - 3$.

Let $s = 5$, we have two possible R-templates. The first is a 3R-template with two medium Seifert circles and the insertion of one small Seifert circle. We will perform the $\theta = 1$ insertion operation on either medium Seifert circle to get 1 small Seifert circle and 3 medium Seifert circles as shown in Figure 4.3.

There are $f = c(D) - 2(2j) - 2\theta = c(D) - 6$ free crossings and $b = 2 + \theta = 3$ insertion boxes to distribute the free crossings. The result is that there are $\binom{b+f-1}{b-1}=$

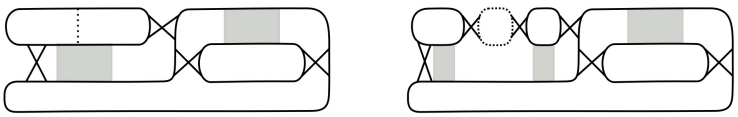

Figure 4.3: A 3R-Template shown with one insertion of a small (dashed) Seifert circle and three insertion boxes

$\binom{c(D)-4}{2}$ 3R-templates with 5 Seifert circles. Now insert the $\theta = 1$ small Seifert circle into one of the two medium Seifert circles, and we have $\binom{2+\theta-1}{2-1}=\binom{2}{1}=2$ ways to do so, resulting in a total of $2\binom{c(D)-4}{2}$ 3R-templates with 5 Seifert circles.

The second template with $s = 5$ is a 5R-template, with 4 medium Seifert circles and $\theta = 0$ insertions. Thus we have $f = c(D) - 8$ and $b = 4$, and a total of $\binom{c(D)-5}{3}$ templates of this type. Therefore, $\psi^I_{c(D)}(5) = \binom{c(D)-5}{3} + 2\binom{c(D)-4}{2}$

We will continue to count the Type I Seifert circle $(2j + 1)$R-templates as follows: Each addition of two more medium Seifert circles to the R-template will result in one more insertion box being placed into each previous template plus the addition of a $(2j + 1)$R-template with no insertions. Figure 4.4 shows three possible R-templates for $s = 7$. The computation for $s = 7$ is:

- Two insertions result in a 3R-template with $f = c(D) - 8$, $b = 2 + \theta$, and $\theta = 2$, thus $\binom{2+\theta+f-1}{2+\theta-1}\binom{2+\theta-1}{2-1} = \binom{c(D)-5}{3}\binom{3}{1}$
- One insertion gives a 5R-template with $f = c(D) - 10$, $b = 4 + \theta$, and $\theta = 1$, thus $\binom{4+\theta+f-1}{4+\theta-1}\binom{4+\theta-1}{4-1} = \binom{c(D)-6}{4}\binom{4}{3}$
- Zero insertions in a 7R-template produces $f = c(D) - 12$, $b = 6$, $\theta = 0$, $\binom{b+f-1}{b-1}\binom{b-1}{6-1} = \binom{c(D)-7}{5}\binom{5}{5}$

This gives $\psi^I_{c(D)}(7) = \binom{c(D)-5}{3}\binom{3}{1} + \binom{c(D)-6}{4}\binom{4}{3} + \binom{c(D)-7}{5}\binom{5}{5}$.

Now, let us consider $s = 2j + 1$ Seifert circles. Let $2k$ be the amount of medium Seifert circles in a $(2k + 1)$R-template and $\theta = j - k$, $f = c(D) - 2(2k) - 2\theta = c(D) - 2k - 2j$, and $b = 2k + \theta$. Then we have:

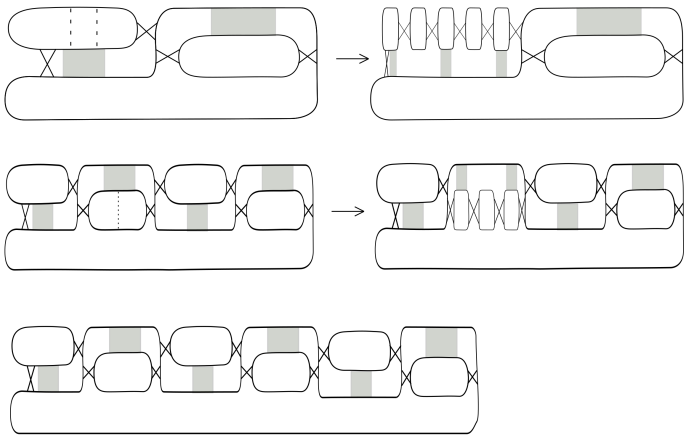

Figure 4.4: Example of R-templates with 7 Seifert circles. Top: A 3R-Template shown with two insertion and four insertion boxes. Middle: a 5R-Template with one insertion and 5 insertion boxes. Bottom: a 7R-Template with no insertions and 6 insertion boxes.

$$\psi^{I}_{c(D)}(s) = \sum_{k=1}^{min[j,\lfloor\frac{c(D)}{2}\rfloor-j]} \binom{c(D)-j-k-1}{k+j-1}\binom{k+j-1}{2k-1} \tag{4.1}$$

4.2 Enumerating Type III links with Seifert circle and crossing number given

Type III links have an even number of Seifert circles $s = 2j$, with one large Seifert circle and $2j-1$ remaining medium and small Seifert circles. We know from the discussion in Chapter 3 that a symmetrical Type III link is its own reversal, and that the R-template cannot differentiate between the two links. Thus when we are counting all Type III links, the algorithm does not recognize the reversal of a symmetrical link as a different link. To resolve this issue, we will need to count the Type III symmetrical links separately. In section 4.3 we will detail how to count the Type III symmetric links.

Beginning with $s = 2$, this decomposition has two Seifert circles and all crossings occur between them. This will give us a 2R-Template with only one insertion box. In this case $\theta = 0$, $b = 1$, $f = c(D) - 2$, thus we have $\psi^{III}_{c(D)}(2) = \binom{c(D)-2}{0}\binom{0}{0} = 1$

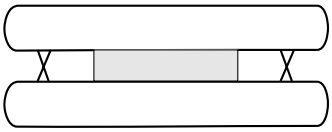

Figure 4.5: Example of a 2R-Template

Using the same R-Template techniques from the Type I's we have for $s = 2j$ there are $2k-1$ medium Seifert circles for each $(2k)$R-template, $\theta = j-k$, $b = (2k-1)+(j-k) = k+j-1$, and $f = c(D)-2(2k-1)-2(j-k) = c(D)-2k-2j+2$,

$$\psi^{III}_{c(D)}(s) = \sum_{k=1}^{min[j,\lfloor\frac{c(D)+2}{2}\rfloor-j]} \binom{c(D)-j-k}{k+j-2}\binom{k+j-2}{2k-2} \tag{4.2}$$

Using the fact that $s = 2j+1$ for $\psi^{I}_{c(D)}(s)$ and $s = 2j$ for $\psi^{III}_{c(D)}(s)$, courtesy of Y. Diao [29] the formulas above can consolidate to:

$$(\psi^{I}_{c(D)} \cup \psi^{III}_{c(D)})(s) = \sum_{k=1}^{min\{\lceil\frac{s-1}{2}\rceil,\lfloor\frac{c(D)}{2}\rfloor-\lfloor\frac{s-1}{2}\rfloor\}} \binom{c(D)-\lfloor\frac{s+1}{2}\rfloor-k}{k+\lfloor\frac{s-1}{2}\rfloor-1}\binom{k+\lfloor\frac{s-1}{2}\rfloor-1}{2k-\frac{(-1)^s+1}{2}-1} \tag{4.3}$$

4.3 Enumerating the Type III symmetrical links with s Seifert circles and crossing number $c(D)$

We now need to address the symmetrical links to add to our count of the $(2j)$R-templates. To do this we will split our templates in half and allocate the insertions and free crossings to one half, then the other half will fill out in a symmetrical manner as shown in Figure 4.6.

The free crossings for Type III is given by $f = c(D)-2k-2j+2$, which will result in four different cases:

Case 1: $c(D)$-odd, θ-odd. This is not possible since an odd number of insertions

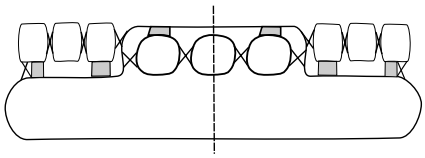

Figure 4.6: Example of splitting a Type III symmetrical link

would result in a center Seifert circle with no free crossings, thus the free crossings would have to distribute half on the left and half on the right, meaning f would be even, but if $c(D)$ is odd, then so is f, so $c(D)$ cannot be odd.

Case 2: $c(D)$-even, θ-odd. There are an odd number of insertions and an odd number $(2j-1)$ of remaining Seifert circles (see Figure 4.6). Splitting the template down the middle, we see that for $2k-1$ medium Seifert circles, there are $k-1$ spots to place the insertions. In addition, we have to place the insertions in such a way to make sure that the insertions are symmetrical on both sides, thus for $\theta = j-k$, there are $\frac{\theta+1}{2}$ insertions we can put on one side. This means there are $\binom{(\theta+1)/2+(k-1)-1}{(\theta+1)/2-1} = \binom{(j+k-1)/2-1}{(j-k+1)/2-1}$ ways to place the insertions in a symmetrical manner.

Since $c(D)$ is even, then f is also even and there are $f = c(D)-2(2k-1)-2(j-k) = c(D)-2k-2j+2$ free crossings after the insertions and $b = j+k-1$ insertion boxes to place the free crossings, dividing each by two gives

$$\binom{(j+k-1)/2+(c(D)-2k-2j+2)/2-1}{(j+k-1)/2-1} = \binom{(c(D)-j-k+1)/2-1}{(j+k-1)/2-1}$$

Case 3: $c(D)$-even, θ-even. Similar to case 2, there are $2k-1$ medium Seifert circles and $k-1$ spots to place the insertions. Since $\theta = j-k$ is even, we have to place the insertions in such a way to make sure that the insertions are symmetrical on both sides, this means there are $\frac{\theta+2}{2}$ insertions we can put on one side. This gives $\binom{(\theta+2)/2+(k-1)-1}{(\theta+2)/2-1} = \binom{(j+k)/2-1}{(j-k)/2}$ ways to place the insertions in a symmetrical manner.

There are $f = c(D)-2(2k-1)-2(j-k) = c(D)-2k-2j+2$ free crossings leftover after the insertions and $b = j+k-1+1$ insertion boxes to place the free crossings (after adding the middle box to place free crossings), dividing each by two

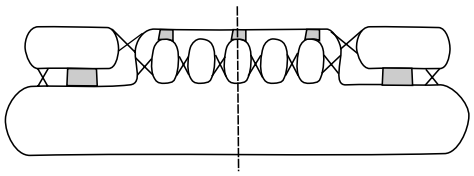

Figure 4.7: Example of splitting a Type III symmetrical link with an even number of insertions

gives $\binom{(j+k)/2+(c(D)-2k-2j+2)/2-1}{(j+k)/2-1}=\binom{(c(D)-j-k)/2}{(j+k)/2-1}$

Case 4: $c(D)$-odd, θ-even. This case is similar to case 3, since $c(D)$ is odd, one of the free crossings will be the middle crossing in the middle box. Thus $f = c(D) - 2k - 2j + 1$, so we have $\binom{(j+k)/2+(c(D)-2k-2j+1)/2-1}{(j+k)/2-1}=\binom{(c(D)-j-k+1)/2-1}{(j+k)/2-1}$

Summarizing the cases listed above, we have the Type III Symmetrical with $2j$ Seifert circles and with $\theta = j - k$:

$$
\begin{aligned}
& \psi^{IIIS}_{c(d)}(s) \\
= & \begin{cases}
\sum_{k=1}^{min\{j,\lfloor\frac{c(D)}{2}\rfloor-j\}} \binom{\frac{c(D)-j-k}{2}}{\frac{j+k}{2}-1}\binom{\frac{j+k}{2}-1}{\frac{j-k}{2}}, & c(D) \text{ even, } \theta \text{ even} \\
\sum_{k=1}^{min\{j,\lfloor\frac{c(D)}{2}\rfloor-j\}} \binom{\frac{c(D)-j-k+1}{2}-1}{\frac{j+k}{2}-1}\binom{\frac{j+k}{2}-1}{\frac{j-k}{2}}, & c(D) \text{ odd, } \theta \text{ even} \\
\sum_{k=1}^{min\{j,\lfloor\frac{c(D)}{2}\rfloor-j\}} \binom{\frac{c(D)-j-k+1}{2}-1}{\frac{j+k-1}{2}-1}\binom{\frac{j+k-1}{2}-1}{\frac{j-k-1}{2}}, & c(D) \text{ even, } \theta \text{ odd} \\
0, & n \text{ odd, } \theta \text{ odd}
\end{cases} \\
= & \frac{1+(-1)^{c(D)(j-k)}}{2} \sum_{k=1}^{min\{j,\lfloor\frac{c(D)}{2}\rfloor-j\}} \binom{\lfloor\frac{c(D)-j-k+2}{2}\rfloor-1}{\lfloor\frac{j+k}{2}\rfloor-1}\binom{\lfloor\frac{j+k}{2}\rfloor-1}{\lfloor\frac{j-k}{2}\rfloor}.
\end{aligned}
$$

Furthermore, this can be stated as [29]

$$
\psi^{IIIS}_{c(d)}(s) = \left(\frac{(-1)^s+1}{2}\right) \sum_{j=1}^{\min\{\lfloor\frac{s}{2}\rfloor,\lfloor\frac{n}{2}\rfloor+1-\lfloor\frac{s}{2}\rfloor\}} \left(\frac{(-1)^{(j+\lfloor\frac{s}{2}\rfloor)n}+1}{2}\right) \binom{\lfloor\frac{n}{2}\rfloor-\lceil\frac{j+\lfloor\frac{s}{2}\rfloor}{2}\rceil}{\lfloor\frac{j+\lfloor\frac{s}{2}\rfloor}{2}\rfloor-1}\binom{\lfloor\frac{j+\lfloor\frac{s}{2}\rfloor}{2}\rfloor-1}{j-1}. \tag{4.4}
$$

In table 4.1, we list the total Type I and III links separately for each $c(D)$. We

then add them together in the third column and finally in our last column we list out the enumeration of the Type III symmetric links. Notice that for for $c(D) = 2n$, $\psi^{IIIS}_{c(d)} = 2^{n-1}$, and for both $\psi^{I}_{c(D)} + \psi^{III}_{c(D)}$ and $\psi^{IIIS}_{c(d)}$ (where $c(D) = 2n+1$) the resulting sequence is one known as the Jacobsthal Sequence.

Table 4.1: Number of Type I, Type III links and their totals and Type III symmetric for crossing number $c(D)$.

n	$\psi^{I}_{c(D)}$	$\psi^{III}_{c(D)}$	$\psi^{I}_{c(D)} + \psi^{III}_{c(D)}$	$\psi^{IIIS}_{c(d)}$
2	0	1	1	1
3	0	1	1	1
4	1	2	3	2
5	2	3	5	1
6	5	6	11	4
7	10	11	21	3
8	21	22	43	8
9	42	43	85	5
10	85	86	171	16
11	170	171	341	11
12	341	342	683	32
13	682	683	1365	21
14	1365	1366	2731	64
15	2730	2731	5461	43

In Table 4.2, the first row represents number of Seifert circles, s and the first column is the crossing number. The last column is the total number of links with crossing number $c(D)$. The remaining output values are the $\psi^{III}_{c(D)}(s)$ or $\psi^{I}_{c(D)}(s)$ respectively.

We are now able to determine $s(D)$, the average number of Seifert circles for any given $c(D)$. However, calculating $g(D)$ also requires that we know the number of components in our link. In order for this to occur, we must be able to differentiate which rational links have only one component and which have two. That will be the goal of our next chapter.

Table 4.2: Each number in the $(c(D), s)$ position represent the total number of links with Seifert circle s and crossing number $c(D)$

$c(D)/s$	2	3	4	5	6	7	8	9	10	11	12	13	14	$\lvert\Lambda_{c(D)}\rvert$
4	2	1	2											5
5	2	2	2											6
6	2	3	6	2	2									15
7	2	4	8	6	4									24
8	2	5	14	13	12	3	2							51
9	2	6	18	24	24	12	4							90
10	2	7	26	40	52	34	20	4	2					187
11	2	8	32	62	90	80	52	20	6					352
12	2	9	42	91	158	166	140	70	30	5	2			715
13	2	10	50	128	246	314	302	200	98	30	6			1386
14	2	11	62	174	382	553	630	496	310	125	42	6	2	2795
15	2	12	72	230	552	920	1176	1106	800	420	164	42	8	5504

CHAPTER 5: DETERMINING THE NUMBER OF COMPONENTS AND AVERAGE GENUS

The formula for the average genus $g(D)$ of a link or knot with crossing number $c(D)$ is given as $2g(D) = c(D) - s(D) - \mu(D) + 2$. In the previous chapter we provided the computations necessary to determine the value of $s(D)$, the average number of Seifert circles, for any given $c(D)$. In this chapter we will prove how to ascertain if a rational link has $\mu(D) = 1$ or $\mu(D) = 2$ component(s) and then compute the average genus for all rational links. In this chapter, we will specifically refer to a knot as a link with one component while a link will have exactly two components.

Theorem 5.0.1. *A $(2j)$R-template is a link and a $(2j+1)$R-template is a knot.*

Proof. Let $j = 1$ and $\mu(D)$ be the number of components for any oriented rational link D. Starting with a standard 2R-template, we can see from the projection that there are two components.

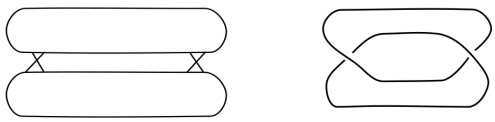

Figure 5.1: A 2R-template is a link

An insertion of small Seifert circle into the 2R-Template will create what we will call a *parity crossing* similar to the one on the left of Figure 5.2, which will not change the number of components since the incoming and outgoing strand remain on the same level (and thus in the same component). Thus the addition of a parity

crossing will not change $\mu(D)$. This will be true for the insertion of any number of Seifert circles, as illustrated in Figure 5.3.

Figure 5.2: Left: Example of a parity crossing. Right: example of a non-parity crossing which will cause the number of components to change.

Note the addition of each non-parity crossing will cause the number of components in L to increase by one. Thus a knot with one component will increase to two components with the introduction of a non-parity crossing. However, since rational links in general cannot have more than two components, the addition of a non-parity crossing to a link will result in a knot. Thus the addition of each non-parity crossing will alternate the number of components between $\mu(D) = 1$ and $\mu(D) = 2$.

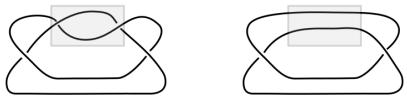

Figure 5.3: Left: The insertion of a small Seifert circle into a 2R-template results in the same number of components as a 2R-template (right)

We can see in Figure 5.4 that for any $(2j)$R-template, the addition of medium Seifert circles results in more parity crossings and $\mu(D)$ will remain unchanged. Similarly, the insertion of a small Seifert circle will result in another parity crossing. Therefore the insertion of Seifert circles will not change the number of components.

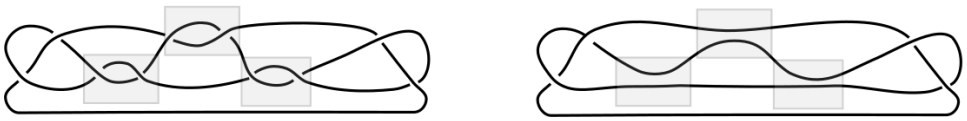

Figure 5.4: Left: A 6R-template adds more medium Seifert circles and thus more parity crossings that result in a link (right)

A similar argument can be made for the $(2j+1)$R-Templates. Let $j = 1$, then the 3R-Template is a knot with one component. Each insertion of medium or small Seifert circles will result in $(2j+1)$R-Templates with additional parity crossings and the number of components will remained unchanged.

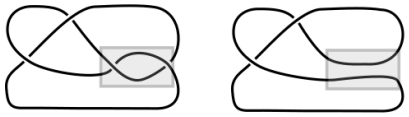

Figure 5.5: Left: A 3R-template results in one parity crossing that can be realized as a knot.

Therefore $s = 2j$ results in a link and $s = 2j+1$ is realized as a knot. □

Theorem 5.0.2. *Let s be the number of Seifert circles in an R-decomposition and $c(D)$ be the number of crossings, then for $s + c(D) = 0\text{mod}2$, L is a link ($\mu(D) = 2$) and for $s + c(D) = 1\text{mod}2$, L is a knot ($\mu(D) = 1$).*

Proof. Consider the R-Templates $s = 2j$ and $s = 2j+1$. Let $f = 1$ and $j = 1$, then for the 2R-template, we have added one non-parity crossing, resulting in a knot. Using the same argument for a 3R-template, the addition of one non-parity crossing will result in a link.

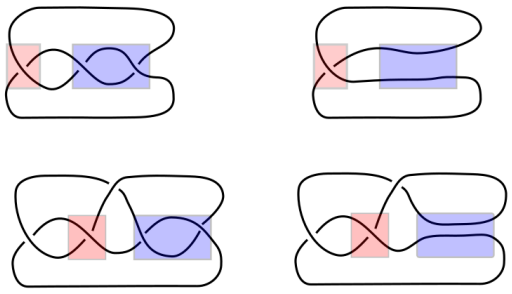

Figure 5.6: Top: A 2R-template with 1 free crossing results in a knot Bottom: a 3R-template with $f = 1$ results in a link

Let $s = 2j$ (or $2j + 1$) with free crossings f distributed among b insertion boxes. Each box will have an even or odd number of free crossings. If the box has an even number of free crossings, then $\mu(D)$ will remain unchanged. However, if a box has an odd number of crossings, the parity will change. Since a rational link can only have one or two components, the parity will alternate between $\mu(D) = 1$ and $\mu(D) = 2$. If f is even, there will be an even number of switches, keeping the parity unchanged, when f is odd there is an odd number of switches, resulting in a change in parity.

Since $c(D)$ is odd (even) if f is odd(even), then we have for $s + c(D) = 0\text{mod}2$, L is a link ($\mu(D) = 2$) and for $s + c(D) = 1\text{mod}2$, L is a knot ($\mu(D) = 1$). □

5.1 Determining the R-decomposition using vector notation

As discussed in Chapter 3, the signed vector $[b_1, b_2, ..., b_{2m+1}]$ represents the crossings in the oriented rational link $L(p/q)$. We will again group the consecutive b_j's with the same signs together into blocks, however we will now denote them by B_1, B_2, ..., B_ρ, where $B_1 = (b_1^1, b_1^2, ...b_1^{2q_1})$, $B_2 = (b_2^1, ...b_2^{2q_2+1})$,...$B_\rho = (b_\rho^1, ...b_\rho^z)$.

Also, as previously discussed, we can see that positive crossings in the PS form correspond with Seifert circles outside C and negative crossings correspond to Seifert circles inside C where each block represents a medium Seifert circle, thus the Seifert circle decomposition of the 4-plat is a $(\rho + 1)$R-Template. By analyzing the vector and its blocks, we can determine the number of insertions (thus Seifert circles), free crossings, and the number of components in the 4-plat. The blocks will be determined as follows:

B_1: We defined our Type I and Type III rational links to always start with a positive block, so this medium Seifert circle will be outside C where $|B_1| = 2q_1$. b_1^1 will contain one essential crossing and $b_1^1 - 1$ free crossings. All other $b_1^{2h_1+1}$ in B_1 will be free crossings. Each $b_1^{2h_1} = 2\sigma_{2h_1}$, where $2h_1 \neq 2q_1$ will be even and represent $\theta = \sigma_{2h_1}$ insertions. The last entry, $b_1^{2q_1} = 2\sigma_{2q_1} + 1$, will be odd, with one essential crossing and $\theta = \sigma_{2q_1}$ insertions.

$B_m, 1 < m \leq \rho$: All other blocks in a Type I and all but the last block in a Type III will have an odd length and adhere to the following: If the block only has one entry, then $b_m^1 = 2\sigma_{m_1}$ and will have $2\sigma_{m_1} - 1$ Seifert circles in the block. Otherwise, each even entry in the block are free crossings and the first and last entry in the block follow the same rule as $b_1^{2q_1}$. All other odd entries will act as the insertion entries in B_1.

B_ρ for Type III: The last block in a Type III will have an even number of entries with b_ρ^1 acting as b_1^{2q}, each b_ρ^{2h} are the free crossings and each $b_\rho^{2h+1} = 2\sigma_{\rho_{2h+1}}$ are insertions and finally the last entry will follow the same format as b_1^1.

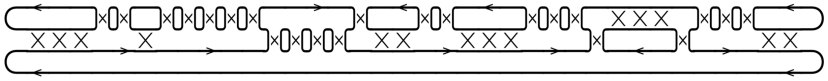

Figure 5.7: The Seifert circle decomposition corresponding to the rational link $[3, 2, 1, 5, -4, 1, 2, 2, 3, 3, -1, -3, -1, 3, 2]$.

In the example above, we see that this is a 6R-template, the first block is $B_1 = [3, 2, 1, 5]$, there are $(3 - 1) + 1 = 3$ free crossings and $(1 + 2 + 5) - 1 = 7$ Seifert circles. The second block has no free crossings and $4 - 1 = 3$ Seifert circles. B_3 has $2 + 3 = 5$ free crossings and $(1 + 2 + 3) - 1 = 5$ Seifert circles. B_4 had 3 free crossings and 1 Seifert circle and B_5 has $2 - 1 = 1$ free crossings and $(3 + 1) - 1 = 3$ Seifert circles. For this link $f = 12$ and $s = 20$.

Using Theorem 5.0.2, we can determine if the 4-plat in vector form is a link or a knot. The 4-plat will have a $(\rho + 1)$R-template. Since any additional Seifert circles inserted will not change the number of components, we can substitute the value of $\rho + 1$ in for s in 5.0.2. We can use the value of f or $c(D) = \sum_{i=1}^{2m+1} a_i$ to complete our analysis. In this example, we have a $\rho + 1 = 6$ with $c(D) = 36$, so this is a link.

5.2 Average Genus of link L with crossing number $c(D)$.

The genus of an oriented link is given by $g(D) = \dfrac{c(D) - s(D) - \mu(D) + 2}{2}$. Given $c(D)$, we can now find the average genus of knots $g^{\kappa}_{c(D)}(D)$ and links $g^{l}_{c(D)}(D)$ and also determine a weighted average for the genus using

$$g_{c(D)}(D) = \frac{g^{\kappa}_{c(D)}(D) * |\kappa_{c(D)}| + g^{l}_{c(D)}(D) * |l_{c(D)}|}{|\Lambda_{c(D)}|}$$

For example, let $c(D) = 9$, then we know when s is odd $\mu(D) = 2$ and when s is even $\mu(D) = 1$. The average $s(D)$ when $\mu(D) = 2$ is $s^{l}_{9}(D) = \dfrac{6 * 3 + 24 * 5 + 12 * 7}{42} = \dfrac{37}{7} = 5.2857$. The average genus is given by $g^{l}_{9}(D) = \dfrac{c(D) - s^{l}_{9}(D) - \mu(D) + 2}{2}$ which will be 1.85714. When $\mu(D) = 1$, the average is $s^{\kappa}_{9}(D) = \dfrac{2 * 2 + 18 * 4 + 24 * 6 + 4 * 8}{48} = \dfrac{21}{4} = 5.25$. The average genus is $g^{\kappa}_{9}(D) = 2.375$. Thus the weighted average genus for $c(D) = 9$ is

$$g_{9}(D) = \frac{2.375 * 48 + 1.857 * 42}{90} = 2.133333$$

.

Experimental data from Dunfield [1] suggests that the genus of a knot grows linearly with respect to $c(D)$. Cohen determined the average genus of a knot approaches $c(D)/4 + 1/12$ [10]. Using the data from our findings, our analysis finds a linear model is reasonable for knots and links.

Table 5.1: In the table, $s_k(D)$ ($s_l(D)$) represents the average number of Seifert circles for all knots (links) with crossing number $c(D)$. Similarly, $g_k(D)$ ($g_l(D)$) represents the average genus for all knots (links). $g(D)$ is the weighted average and $|\Lambda_{c(D)}| = |k| + |l|$ is the total number of rational links with crossing number $c(D)$.

$c(D)$	$s_k(D)$	$g_k(D)$	$s_l(D)$	$g_l(D)$	$g(D)$	$\lvert k\rvert$	$\lvert l\rvert$	$\lvert\Lambda_{c(D)}\rvert$
4	3	1	3	0.5	0.6	1	4	5
5	3	1.5	3	1	1.33333	4	2	6
6	3.8	1.6	4	1	1.2	5	10	15
7	4.2857	1.8571	4.2	1.4	1.6667	14	10	24
8	4.8095	2.0952	4.9333	1.5333	1.7647	21	30	51
9	5.25	2.375	5.2857	1.857	2.13333	48	42	90
10	5.8235	2.5882	5.88241	2.05882	2.2995	85	102	187
11	6.3077	2.8462	6.3176	2.34121	2.6023	182	170	352
12	6.8299	3.08504	6.8556	2.5722	2.8168	341	374	715
13	7.3125	3.3438	7.3284	2.8358	3.0938	704	682	1386
14	7.8322	3.5839	7.84333	3.0783	3.3252	1365	1430	2795

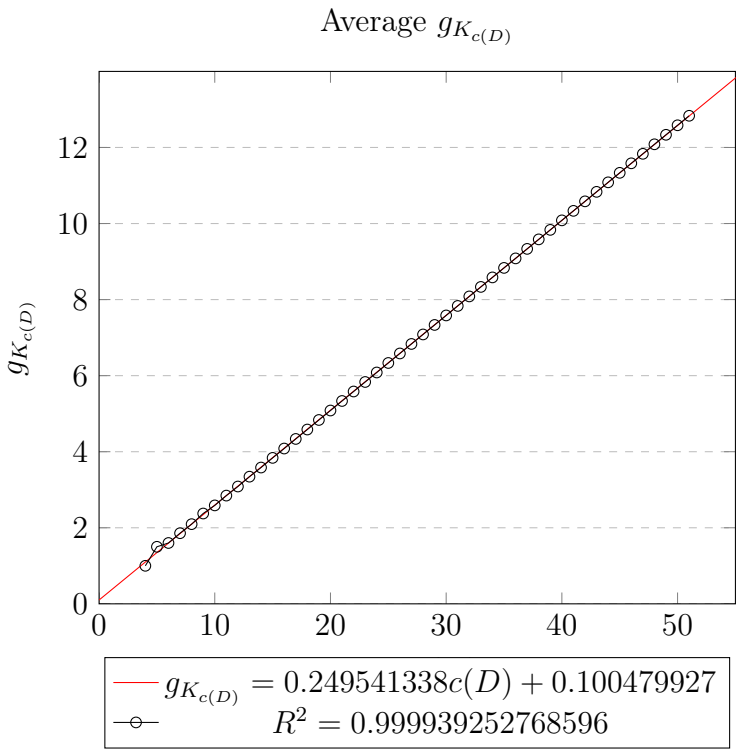

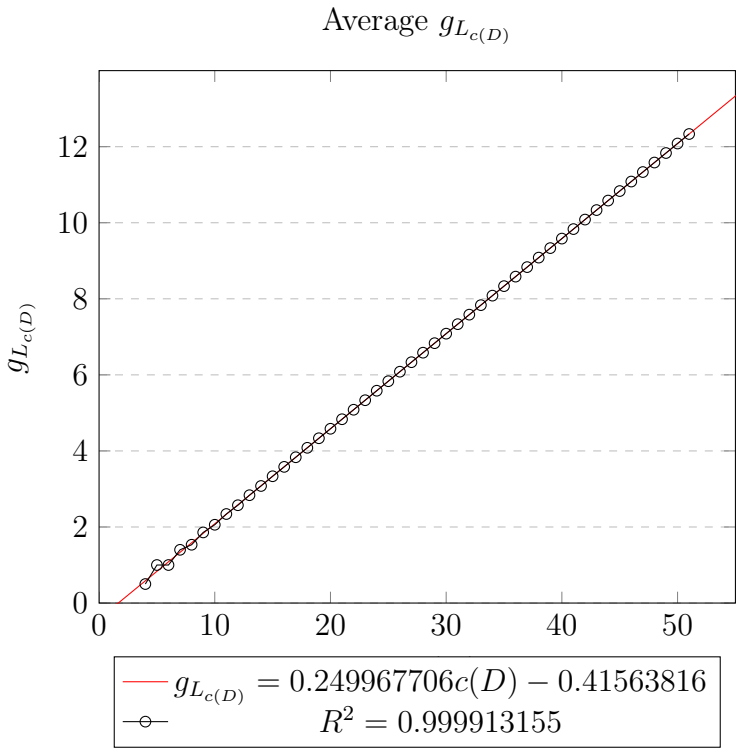

The models indicate a reasonable conjecture that there is a linear relationship between $c(D)$ and $g_{K_{c(D)}}$ ($g_{L_{c(D)}}$) with at R^2 value of 0.999939253 (0.999913155).

An analysis of the spread of the average genus $g_{c(D)}$ also produces a strong linear relationship between $c(D)$ and $g_{c(D)}$ indicating that as $c(D) \to \infty$, $g_{c(D)} = 0.25c(D)$ with $R^2 = 0.999739351$.

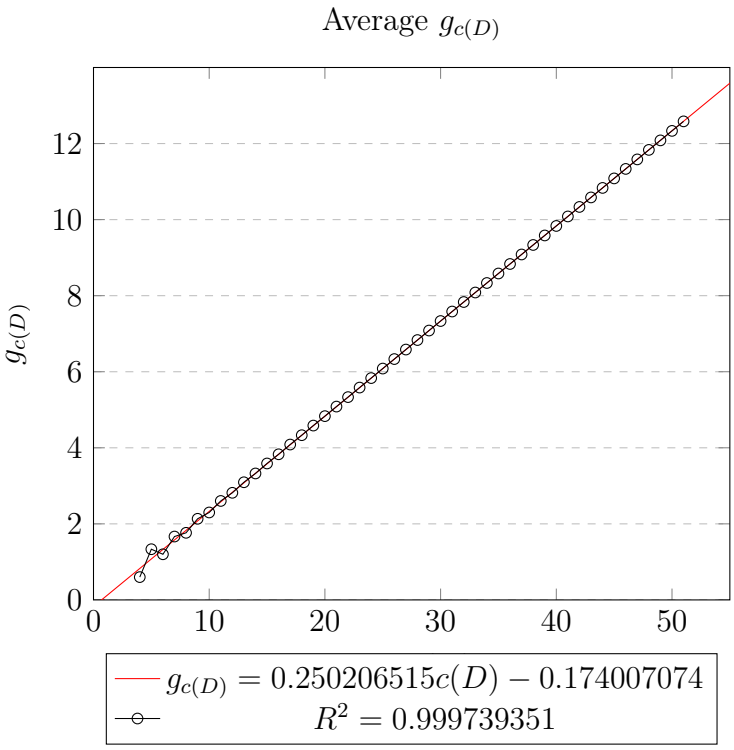
Average $g_{c(D)}$
$g_{c(D)}$
0
2
4
6
8
10
12
0
10
20
30
40
50
$g_{c(D)} = 0.250206515c(D) - 0.174007074$
$R^2 = 0.999739351$

CHAPTER 6: FUTURE WORK AND CONCLUSION

Our work on the enumeration of oriented rational links has led us to research the possibility of enumerating a larger class of links called the Montesinos links. In this chapter, we will define some properties of Montesinos links and outline our progress thus far on enumerating Montesinos links of deficiency zero.

6.1 Montesinos Links

A *Montesinos link* $\mathcal{L} = \mathcal{M}(\beta_1/\alpha_1, ...\beta_k/\alpha_k, e)$ is a link where each tangle A_j corresponds to each β_j/α_j where $|\beta_j/\alpha_j| < 1$ for $1 \leq j \leq k$ and e stands for an arbitrary number of half twists, as shown in Figure 6.1. Since we are interested in alternating Montesinos links, all β_j/α_j will be required to have the same signs and that will be matched by the sign of e, which is not to be confused with the sign of the individual crossings.

The Classification Theorem states that Montesinos links with $k \geq 3$ rational tangles are classified by the ordered set of fractions $(\frac{\beta_1}{\alpha_1} mod 1, ... \frac{\beta_k}{\alpha_k} mod 1)$ and are considered equivalent up to cyclic permutations and reversal of order, together with the rational number $e_0 = e - \sum_{j=1}^{r} \frac{\beta_j}{\alpha_j}$ [19].

For each tangle A_j, β_j/α_j will consist of the standard continued fraction with an odd number of positive entries, thus it will be of the form $(a_1^j, ..., a_{2q_j+1}^j)$, allowing for $a_{2q_j+1}^j$ to equal one to make the vector have an odd length.

The closure of each rational tangle will be obtained by connecting the NW and SW strands and the NE and SE strands, resulting in a denominator closure $D(A_j)$ of the tangle A_j. Requiring that $\beta_j/\alpha_j < 1$ means that each rational tangle will begin with a vertical row of twists.

Each oriented Montesinos link will be drawn with the top strand oriented from right to left. Note that if $k = 2$, then our link is actually a two bridge link and the counting for those have been completely determined as outlined in Chapter 3.

Assigning orientation to each tangle results in the signed vector $(b_1^j, .., b_{k_j}^j, .., b_{2q_j+1}^j)$, where each $|b_m^j| = a_m^j$. The notation $A_j(b_1^j, .., b_{k_j}^j, .., b_{2q_j+1}^j)$ is used to denote the tangle A_j and the signed vector associated with it. We will refer to the first set of vertical twists in each tangle A_j as b_1^j.

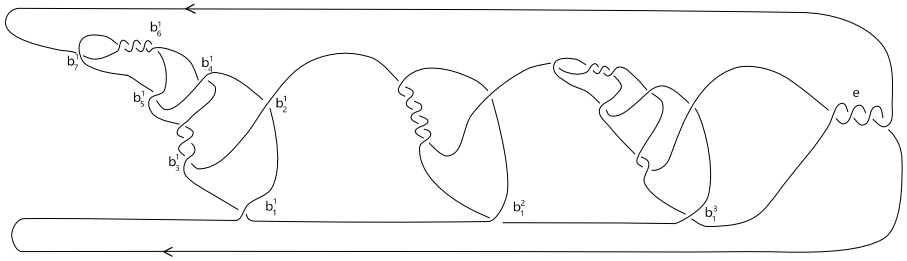

Figure 6.1: Montesinos link $\mathcal{M}(50/89, 6/11, 32/55, 4)$ with orientation.

Based on the assigned orientation of the top strand, the Seifert circle decomposition of $\mathcal{L}$ will have one or two huge Seifert circles containing the top and bottom strands. In addition, there will be large Seifert circles consisting of the strands that are entering/exiting one or more tangles. Finally there will be medium and small Seifert circles within each tangle.

Figure 6.2 shows the eight possible ways arcs can enter and exit each tangle [27] to create huge and large Seifert circles. Within each tangle, there could be medium and small Seifert circles, however for now we will focus on these two specific strands. First, consider options (vi) and (viii), each tangle has a denominator closure and the NE-SE and NW-SW strings meet at the first crossing b_1^j. This means that if these two strands belong to two different Seifert circles then they must have parallel orientation. However, figures (vi) and (viii) do not have parallel orientation, and therefore these

two options are not possible. Since the orientation of the top strand is assigned as right to left, option (iii) is also not possible. We will define three *Seifert Parities* from the remaining possibilities. A tangle is of Seifert Parity 1 if the Seifert circles entering and exiting decomposes like (i), Seifert Parity 2 if it decomposes as (ii) or (iv) and Seifert Parity 3 if it presents as (v) or (vii). We can further classify $\mathcal{L}$ into three classes.

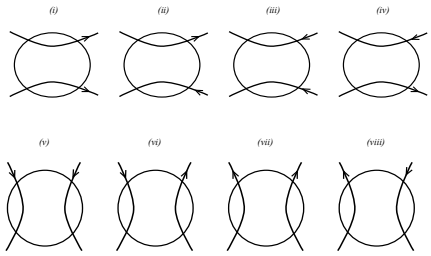

Figure 6.2: Eight options for tangles consisting of three different parities

Class M1: An M1 link has the top and bottom strands running parallel (from right to left) as shown in Figure 6.1, thus there are two huge Seifert circles and all tangles A_j are of Seifert Parity 1 with all crossings in e negative. All tangles will decompose as (i).

Class M2: The bottom strand has orientation from left to right and thus the top and bottom strands belong to two huge Seifert circles. Each A_j will be of Seifert Parity 2 and thus will decompose as (ii) in Figure 6.2 with $e = 0$.

Class M3: The top and bottom strand belong to one huge Seifert circle. A link $\mathcal{L}$ is a class M3 link if and only if at least one A_j is of Seifert Parity 3 and all crossings in e are positive.

6.2 M1 Montesinos Links of Deficiency Zero

Let $\mathcal{L}(d)$ be the deficiency of link $\mathcal{L}$. The requirement that $\mathcal{L}(d) = 0$ means that each A_j must be deficiency zero. The purpose of this next section is to determine the restrictions on each A_j in a class M1 link to guarantee $d(\mathcal{L}) = 0$.

First note that since $e \leq 0$, the crossings in e will smooth horizontally and thus e can be any negative value.

Since each tangle is of Seifert Parity 1, the strands corresponding with SE and SW will enter the tangle in a vertical block as a negative crossing, $b_1^j < 0$ (which will smooth horizontally), to ensure there are no cycles within each tangle, this must be a single crossing and $b_1^j = -1$.

We will call the Seifert circle decomposition of the M1 Montesinos link a M1-decomposition. In the Seifert circle diagram, we will call the large circle containing the long arc on top γ_1 and the large circle containing the bottom long arc γ_2. Each tangle shares one *essential* crossing (b_1^j) between γ_1 and γ_2 as shown in Figure 6.3.

We will call the Seifert circles inside and outside γ_1 medium Seifert circles. Each medium Seifert circle is connected to γ_1 via 2 essential crossings. Any crossings shared between a medium Seifert circle and γ_1 that are not essential are the free crossings.

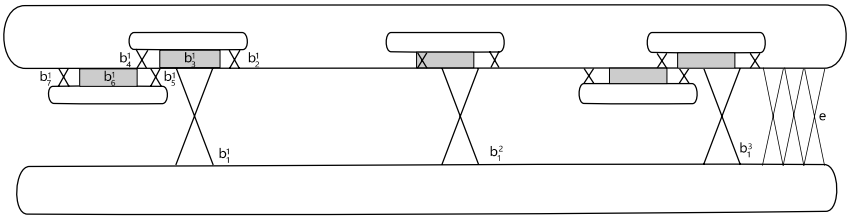

Figure 6.3: M1-decomposition of a zero deficiency M1 link

Since all tangles must be of Seifert parity 1, this will require that $b_2^j > 0$ will consist of essential crossings. Thus b_2^j has two possible values; if the medium Seifert circle has free crossings then $b_2^j = 1$, if not, then $b_2^j = 2$. If $b_2^j = 1$, then $b_3^j > 0$ will be free crossings and $b_4^j = 1$ will be an essential crossing. These three components comprises the first block and creates a medium Seifert circle which lies within γ_1.

The next block will consist of components that will construct a medium Seifert circle outside of γ_1. Assuming the medium Seifert circle has free crossings, $b_5^j = -1, b_6^j < 0$,

and $b_7^j = -1$, otherwise the block consists of one component, -2. All subsequent blocks will result in medium Seifert circles alternating inside and outside γ_1. Each block will consist of one value (± 2) or three ($\pm 1, \pm f^j, \pm 1$), where f^j are the free crossings in each block. For our counting purposes, we will require that a block consisting of (± 2) be written as ($\pm 1, 0, \pm 1$).

Referring to the signed vector $(b_1^j, .., b_{k_j}^j, .., b_{2q_j+1}^j)$, where each $|b_m^j| = a_m^j$, the essential crossings will be distributed so that:

Each tangle A_j will share one essential crossing between γ_1 and γ_2, this is the crossing $|b_1^j| = 1$. Thus there are j essential crossings.

Each subsequent set of three components represent a Seifert circle inside then outside of γ_1, which will each have two essential crossings. If $2q_j + 1 = 1\text{mod}3$, then this pattern will hold throughout the tangle. If $2q_j + 1 = 0\text{mod}3$, then the last block will have only two components wherein $b_{2q_j+1}^j$ will consist of free crossing(s) and one essential crossing, as can be seen in the second tangle in Figure 6.3. Otherwise, each block must have three components, thus $2q_j + 1 \neq 2\text{mod}3$. All of the blocks will contribute a total of $\sum_{i=1}^{j}(2\lfloor\frac{2q_i+1}{3}\rfloor)$ essential crossings, resulting in a total of $\sum_{i=1}^{j} 1 + (2\lfloor\frac{2q_i+1}{3}\rfloor)$ essential crossings.

All free crossings will be distributed throughout the $k_j = 3\text{mod}6$ and $k_j = 0\text{mod}6$ components of the vector, as well as e. There will be $2 + \sum_{i=1}^{j}\lfloor\frac{2q_i+1}{3}\rfloor$ Seifert circles and there will be $1 + \sum_{i=1}^{j}\lfloor\frac{2q_i+1}{3}\rfloor$ insertion boxes to distribute the free crossings.

Let n be the total number of crossings, j be the number of tangles and k be the total number of medium Seifert circles. Then there are a total of $2k + j$ essential crossings. Let f be the number of free crossings, then $n = f + 2k + j$, or $f = n - 2k - j$ where $n \geq 9$, $3 \leq j \leq k$.

The Classification Theorem states that Montesinos links are isotopic up to reversal of order and cyclic permutation thus without loss of generality we will let the first tangle A_1 be the tangle with the least number of medium Seifert circles. There are j

tangles and each must have at least one medium Seifert circle and there are k medium Seifert circles, thus we can distribute the remaining $k-j$ Seifert circles and there are $\binom{j+(k-j)-1}{j-1}=\binom{k-1}{j-1}$ ways to do so.

Free crossings can be placed in e or between essential crossings for each medium Seifert circle, thus there are $k+1$ spots to place free crossings. Therefore $\binom{(k+1)+(n-2k-j)-1}{(k+1)-1}$ $= \binom{n-k-j}{k}$. Let $|R^1_{n_j}|$ be the number of M1 Montesinos links where $\mathcal{L}(d) = 0$, then

$$|R^1_{n_j}| = \sum_{j=3}^{\lfloor \frac{n}{3} \rfloor} \sum_{k=j}^{\min[j, \lfloor \frac{n-j}{2} \rfloor]} \binom{k-1}{j-1} \binom{n-k-j}{k}$$

6.3 Remaining Classes

The M2 class of Montesinos links contain all A_j's with Seifert Parity 2, thus similarly to M1 the SE and SW strands entering the tangle must be a negative vertical crossing, thus $b^j_1 = -1$. The next crossing will be a horizontal crossing with $b^j_2 < 0$. However, since $j \geq 3$ and there are two huge Seifert circles with antiparallel orientation, then each tangle A_j must create at least one (large) Seifert circle in between the two huge Seifert circles. The existence of large Seifert circles between the two huge ones will result in cycle(s) with lone crossings. However, the requirement that $\mathcal{L}(d) = 0$ dictates that there are no cycles in the Seifert circle decomposition. Therefore, there are no M2 links of deficiency zero.

The class M3 links have a significantly more complicated structure. Because the top and bottom strand connect to one huge Seifert circle γ, tangles within γ are only limited to the requirement that one be of Seifert Parity 3, thus tangles within γ can be any combination of (v), (vii), (ii) or (iv). This is a topic that can be further considered in the future. Once done, we would like to get a bound on the deficiency zero links of class M1 and M3. We can then expand our research to higher deficiency values.

REFERENCES

[1] N. Dunfield, "Random knots: a preliminary report." https://nmd.pages.math.illinois.edu/slides/random$_k$*nots.pdf*, 2014. *Accessed* : $20222 - 16$.

[2] M. Cohen, "A lower bound on the average genus of a 2-bridge knot," *arXiv preprint arXiv:2108.00563*, 2021.

[3] Y. Diao, M. L. Finney, and D. Ray, "The number of oriented rational links with a given deficiency number," *Journal of Knot Theory and Its Ramifications*, vol. 30, no. 09, p. 2150065, 2021.

[4] S. A. Wasserman, J. M. Dungan, and N. R. Cozzarelli, "Discovery of a predicted dna knot substantiates a model for site-specific recombination," *Science*, vol. 229, no. 4709, pp. 171–174, 1985.

[5] K. Murasugi, J. H. Przytycki, and J. Przytycki, *An index of a graph with applications to knot theory*, vol. 508. American Mathematical Soc., 1993.

[6] R. H. Crowell, "Genus of alternating link types," *Annals of Mathematics*, pp. 258–275, 1959.

[7] K. Murasugi, "On the genus of the alternating knot, i," *Journal of the Mathematical Society of Japan*, vol. 10, no. 1, pp. 94–105, 1958.

[8] T. Kanenobu, "Genus and kauffman polynomial of a 2-bridge knot," *Osaka Journal of Mathematics*, vol. 29, no. 3, pp. 635–651, 1992.

[9] D. Gabai, "Genera of the alternating links," *Duke mathematical journal*, vol. 53, no. 3, pp. 677–681, 1986.

[10] M. Cohen and A. M. Lowrance, "The average genus of a 2-bridge knot is asymptotically linear," *arXiv preprint arXiv:2205.06122*, 2022.

[11] C. Ernst and D. Sumners, "A calculus for rational tangles: applications to dna recombination," in *Mathematical Proceedings of the Cambridge Philosophical Society*, vol. 108, pp. 489–515, Cambridge University Press, 1990.

[12] H. Doll and J. Hoste, "A tabulation of oriented links," *Mathematics of Computation*, vol. 57, no. 196, pp. 747–761, 1991.

[13] J. Hoste, M. Thistlethwaite, and J. Weeks, "The first 1,701,936 knots," *Math. Intelligencer*, vol. 20, no. 4, pp. 33–48, 1998.

[14] C. N. Little, *On knots with a census for order ten*, vol. 7. The Academy, 1885.

[15] C. Ernst and D. Sumners, "The growth of the number of prime knots," in *Mathematical proceedings of the cambridge philosophical society*, vol. 102, pp. 303–315, Cambridge University Press, 1987.

[16] P. R. Cromwell *et al.*, *Knots and links*. Cambridge university press, 2004.

[17] W. S. Massey, *A basic course in algebraic topology*, vol. 127. Springer, 2019.

[18] K. Reidemeister, "Elementare begründung der knotentheorie," in *Abhandlungen aus dem Mathematischen Seminar der Universität Hamburg*, vol. 5, pp. 24–32, Springer, 1927.

[19] G. Burde and H. Zieschang, "Knots," in *Knots*, de Gruyter, 2008.

[20] C. C. Adams, *The knot book*. American Mathematical Soc., 1994.

[21] L. H. Kauffman and S. Lambropoulou, "On the classification of rational knots," *arXiv preprint math/0212011*, 2002.

[22] L. H. Kauffman and S. Lambropoulou, "Classifying and applying rational knots and rational tangles," *Contemporary mathematics*, vol. 304, pp. 223–260, 2002.

[23] H. Schubert, "Knoten mit zwei brücken," *Mathematische Zeitschrift*, vol. 65, no. 1, pp. 133–170, 1956.

[24] J. W. Alexander, "A lemma on systems of knotted curves," *Proceedings of the National Academy of Sciences of the United States of America*, vol. 9, no. 3, p. 93, 1923.

[25] S. Yamada, "The minimal number of seifert circles equals the braid index of a link," *Inventiones mathematicae*, vol. 89, no. 2, pp. 347–356, 1987.

[26] Y. Diao, G. Hetyei, and P. Liu, "The braid index of reduced alternating links," in *Mathematical Proceedings of the Cambridge Philosophical Society*, vol. 168, pp. 415–434, Cambridge University Press, 2020.

[27] Y. Diao, C. Ernst, G. Hetyei, and P. Liu, "A diagrammatic approach for determining the braid index of alternating links," *arXiv preprint arXiv:1901.09778*, 2019.

[28] Y. Diao, "The additivity of crossing numbers," *Journal of knot theory and its Ramifications*, vol. 13, no. 07, pp. 857–866, 2004.

[29] D. Ray and Y. Diao, "The average genus of oriented rational links," *preprint*, 2022.